ohio2/yjp-yjp/yjp-yjp/yjp99907/yjp8202d07z | xppws | 23:ver.3 | 9/4/09 | 10:38 | Msc: jp-2009-055522 | TEID: jem00 | BATID: 00000

Thyroid Hormone Interactions with DMPC Bilayers. A Molecular Dynamics Study

Ariel A. Petruk,[†] Marcelo A. Marti,*[,‡] and Rosa María S. Álvarez*[,†,§]

Instituto Superior de investigaciones Biológicas (CONICET-UNT), Chacabuco 461, San Miguel de Tucumán, Tucumán, T4000CAN, Argentina, Departamento de Química Biológica y Departamento de Química Inorgánica, Analítica y Química Física (INQUIMAE-CONICET), Facultad de Ciencias Exactas y Naturales, Universidad de Buenos Aires, Ciudad Universitaria, Pabellón 2, Buenos Aires, C1428EHA, Argentina, and Instituto de Química Física, Facultad de Bioquímica, Química y Farmacia, Universidad Nacional de Tucumán, San Lorenzo 456, San Miguel de Tucumán, Tucumán, T4000CAN, Argentina

Received: June 13, 2009; Revised Manuscript Received: August 21, 2009

The structure and dynamics of thyroxine (T4), distal and proximal conformers of 3′,3,5-triiodo-L-thyronine (T3d and T3p), and 3,5-diiodo-L-thyronine (T2) upon interaction with DMPC membranes were analyzed by means of molecular dynamics simulations. The locations, the more stable orientations, and the structural changes adopted by the hormones in the lipid medium evidence that the progressive iodine substitution on the β ring lowers both the possibility of penetration and the transversal mobility in the membrane. However, the results obtained for T3d show that the number of iodine atoms in the molecule is not the only relevant factor in the hormone behavior but also the orientation of the single iodine substitution. The electrostatic interactions between the zwitterion group of the hormones with specific groups in the hydrophilic region of the membrane as well as the organization of the alkyl chains around the aromatic β ring of the hormone were evaluated in terms of several radial distribution functions.

Thyroid hormones (THs) exert profound effects on the metabolism, growth, and development of vertebrates. About 97.5% of the circulating THs consists of thyroxine (T4), which is deiodinated at target tissues, yielding 3′,3,5-triiodo-L-thyronine (T3). Other iodothyronines are also formed by the deiodination mechanisms, and these are present in small concentrations in the plasma (Figure 1A). For many years, T3 was considered as the metabolically active hormone because its functions were the only known among those of the other THs. However, more recently, 3,5-diiodo-L-thyronine (T2) and 3′,3-diiodo-L-thyronine (rT2) have also acquired biological relevance.[1−3]

THs are found in the plasma, either bound to plasma proteins or in the free state. Many of these thyroid-hormone-binding proteins have been identified as TH membrane transporters, while others were considered just as "distributor proteins".[4,5] Among the characterized transporters are the L-type amino acid transporters, different members of the organic anion transporting polypeptide (OATP), and the monocarboxylate transporter (MCT) families,[6−9] particularly OATP1C1, MCT8, and MCT10, which were recently identified as highly specific in transporting iodothyronines. On the other hand, it was traditionally assumed that, due to their lipophilic nature, the translocation of thyroid hormones over the plasma membrane of target cells was a process of simple diffusion. Thus, the "free hormone hypothesis" was formulated in 1960 by Robbins and Rall.[10] Years later, by employing electronic spin-resonance techniques, the lateral diffusion of spin-labeled T3 and T4 was reported and it was suggested that the nonionized phenolic−OH group was close to the lipid core of the membrane.[11−13] To gain insight into the mechanisms by which T3 and T4 reach the intracellular compartment, interactions and transmembrane diffusion experiments with liposomes were performed in our laboratory and the results revealed that both hormones could regulate membrane fluidity, similarly to cholesterol, causing an increase of the fluidity in the gel phase and a decrease in the liquid-crystalline state.[14−16] It has also been reported that THs affect the monolayer dipolar organization and the magnitude of this effect was associated with the number of iodine atoms in the hormone molecule. In addition, this effect was postulated like a new nongenomic action of THs at the cellular level.[17] F1

A few years ago, we refocused our interest in understanding these specific hormone−membrane interactions in more detail, analyzing the molecular structures of the TH interaction with phospholipids. In this regard, our vibrational studies by Raman spectroscopy and density functional theory (DFT) calculations allowed us to detect spectral changes observed for T4 and T3 upon binding to phospholipids and to postulate that they are likely due to specific conformational changes adopted by the hormones after inserting into the lipid bilayer, according to their specific steric requirements.[18,19] It is interesting to point out the structure and dynamics of T3, since the single substitution of one iodide atom in the β ring yields two conformers termed as distal (T3d) and proximal (T3p) according to the orientation of the substituent with respect to the α ring (Figure 1). Thus, while crystal structures of T3 show only the T3p conformer,[20] NMR experiments in methanol solution[21] and Raman spectra of T3-phosphatidylcholine mixtures[19] show both conformers in equilibrium. Further interpretations concerning the intimate molecular interactions involved in the transmembrane diffusion processes are difficult due to the lack of information about the structure of biological membranes loaded with THs with atomic resolution.

In the last decades, the molecular dynamics (MD) simulation technique has become an invaluable tool for the study of bimolecular systems. MD offers the possibility of studying the structures and dynamics of biomolecules in an explicit solvent

* To whom correspondence should be sent. marcelo@qi.fcen.uba.ar (M.A.M.); mysuko@fbqf.unt.edu.ar (R.M.S.A.).
[†] Instituto Superior de investigaciones Biológicas (CONICET-UNT).
[‡] Universidad de Buenos Aires.
[§] Universidad Nacional de Tucumán.

10.1021/jp9055522 CCC: $40.75

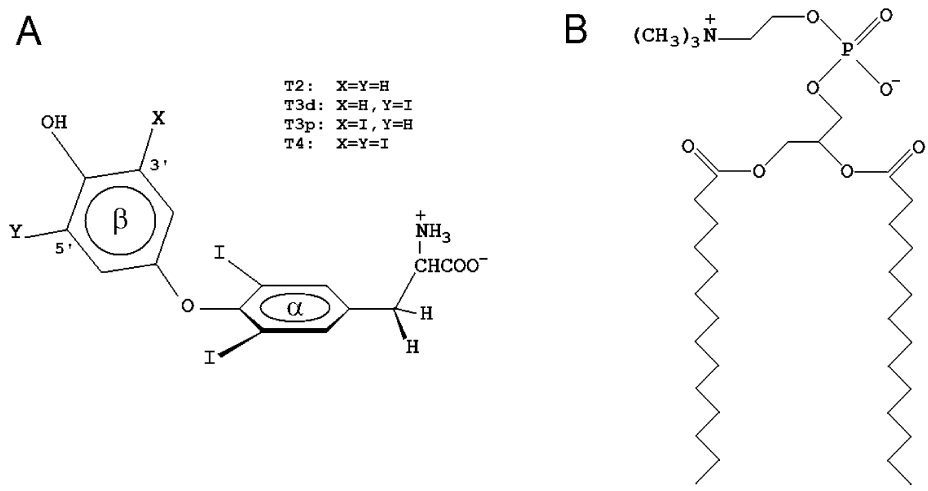

Figure 1. Molecular structures of (A) thyroid hormones and (B) dimyristoylphosphatidylcholine.

environment with atomistic detail in the nanosecond time scale. Particularly interesting are studies showing that MD was able to correctly reproduce the experimental knowledge about the interactions between cholesterol and phospholipids[22−28] as well as the interactions of many other molecules including aromatic amino acids, small polypeptides, and proteins with phospholipid bilayer,[29,30] revealing, in addition, some new information experimentally inaccessible.

In this work, we have analyzed in detail the structure and dynamics of THs upon interaction with phospholipids. MD simulations of TH−membrane complexes, constructed with individual T4, T3d, T3p, and T2 molecules in fully hydrated liquid-crystalline dimyristoylphosphatidylcholine (DMPC) bilayer membranes allowed us to determine the locations and more stable orientations adopted by each TH in the lipid medium. For each TH−membrane complex, 20 ns long equilibrated trajectories were analyzed. The specific interactions derived from these analyses are discussed in terms of possible physiological implications. In addition, structural changes of THs, induced by interactions with the phospholipids, were evaluated and compared with previous experimental results.

Computational Methods

System Setup and Parameters. The initial system used for the simulation consisted of a hydrated dimyristoylphosphatidylcholine bilayer, which was built with 72 ($6 \times 6 \times 2$) DMPC molecules and ~2500 water molecules, based on a previous bilayer structure.[31] Similar membrane dimensions were used to study the partitioning of aromatic amino acid side chains in a dioleoylphosphatidylcholine bilayer constructed with 64 DOPC molecules and 2807 water molecules.[28] The force field parameters and charges for the DMPC molecules where taken from ref 32. Four TH−DMPC complexes were then constructed by including a single T2, T3d, T3p, and T4 molecule in the membrane/water interfacial region in each case. The hormone structures were previously optimized and their point charges determined by applying the restricted electrostatic potential (RESP) formalism[33] using the Gaussian 03 program.[34] These calculations were performed with the HF/6-31g** method for C, H, O, and N atoms of the hormones, while HF/lanl2dz was used for iodine atoms. In order to get the parameters of the hormone molecules suitable to dynamic simulations, the general AMBER force field included in the AMBER package was used.[35] After the system assembling, the DMPC bilayer membrane and the four TH−DMPC complexes were optimized by 250 steps with the AMBER program.[36]

MD Simulations. The equilibration protocol consisted of heating the optimized structures from 0 to 310 K in 0.2 ns, while the volume of the hydrated bilayers was kept constant. Then, constant isotropic pressure simulations were performed for 0.2 ns followed by another 0.2 ns of simulations at constant anisotropic pressure. In order to accelerate the process of hormone incorporation into the membrane, the hormone molecule was gently pulled along the normal to the membrane surface until the β ring was embedded in the hydrocarbon chains and the zwitterionic group left near the hydrophilic head of the lipids. This incorporation process took about 5 ns. At this point, the hormone was released into the lipid medium, and the simulations were allowed to continue until a total time of 30 ns.

In order to extract the geometric parameters of the THs in the absence of lipid interactions, 5 ns long MD simulations were performed for each hormone in water solvent. A single T2, T3d, T3p, and T4 molecule was solvated with water molecules (TIP3P) in an octahedral box of 35 Å radius. The systems were heated from 0 to 310 K at constant volume and isotropic pressure.

All simulations were performed using periodic boundary conditions and the particle mesh Ewald (PME) summation method for treating long-range electrostatic interactions, using the default AMBER parameters. The SHAKE method of constraining hydrogen atoms to their equilibrium positions was also used.[37] A time step of 2 fs and a cutoff distance of 12 Å were used for direct interactions. The Berendsen thermostat[38] was used to keep the temperature constant at 310 K (corresponding to 37 °C, which is above the main phase transition temperature of 23 °C for a pure DMPC bilayer). All MD simulations were performed with the AMBER suite of programs.[36]

Data Analysis. The results described in this paper were obtained from the final 20 ns trajectories of the MD simulations performed for each system. All of the data was analyzed by using the VMD program.[39] In order to verify that the computed membrane reproduces most features of the experimental system, several parameters, which characterize a DMPC membrane, were determined from the simulations and exhaustively compared with those from experimental studies. Thus, the mean surface area/DMPC molecule, the number of *gauche* conformations/alkyl chain, as well as the tilt angles of the head and tail groups of DMPC molecules with respect to the bilayer normal vector (*Z*-axis) were monitored in each system. The mean surface area/DMPC was obtained by dividing the total surface area of the membrane into 36 DMPC molecules present in each leaflet of the bilayer. Orientations of the DMPC head and tail groups were calculated as the average angles between the *Z*-axis

ohio2/yjp-yjp/yjp-yjp/yjp99907/yjp8202d07z | xppws | 23:ver.3 | 9/4/09 | 10:38 | Msc: jp-2009-055522 | TEID: jem00 | BATID: 00000

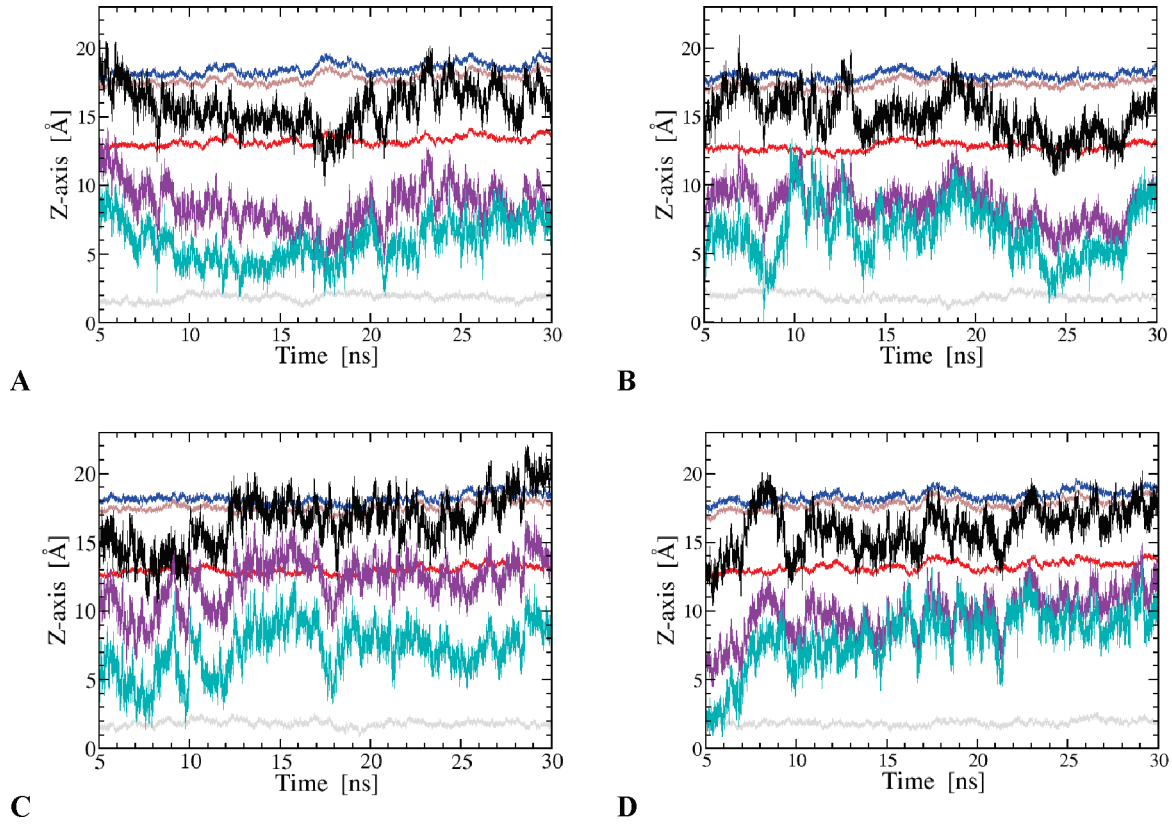

Figure 2. Vertical position (*Z*-axis) of selected THs and DMPC atoms vs time profile in the systems (A) T2-DMPC, (B) T3d-DMPC, (C) T3p-DMPC, and (D) T4-DMPC. DMPC atoms: N (blue), P (brown), carbonyl O (red), and methyl terminal C (gray). TH atoms: carboxylic carbon (black), ether oxygen (violet), and phenol oxygen (turquoise).

and the P−N and C1−C14 vectors, respectively. In order to facilitate the interpretation of the obtained results, it was determined that the origin of the *Z*-axis scale expressed in Å corresponds to the core of the bilayer. In this way, the relative positions of the THs in one monolayer of the membrane were analyzed, and the penetration of each hormone in the lipid medium was evaluated by determining the location of its molecular geometric center, which was calculated by considering arbitrarily only the carbon atoms integrating both aromatic rings and the alanine moiety, with respect to the *Z*-axis. The more stable orientation adopted by each hormone molecule in the lipid was defined as a function of the angles that form the normal vectors to the planes of α and β rings, respectively, with the *Z*-axis of the membrane, and the angles between this last one and the vectors along the distal and proximal molecular bonds in the β ring, respectively. In addition, specific hormone−lipid and hormone−water interactions were analyzed by computing radial distribution functions (RDFs) between pairs of selected atoms.

Results and Discussion

Comparison between Simulated and Experimental Membrane Parameters. ***DMPC Bilayer.*** The hydrated membrane consisted of 36 DMPC molecules on each leaflet and a ratio of 34 water molecules/DMPC. The mean surface area/DMPC of 61 Å^2 was obtained from the simulations, in agreement with those experimental values of 60.0 and 65.4 Å^2 obtained by NMR studies at 303 and 323 K, respectively.[40] The average number of *gauche* rotamers/alkyl chain along the simulation time was 3.5, while a reported value of 3.57 was obtained by Raman spectroscopy at 303 K.[41] Neutron diffraction studies have shown that the average orientation of the lipid head groups in DMPC bilayers is almost parallel to the membrane surface.[42] Moreover, electron spin resonance studies reported a perpendicular orientation of the tail groups with respect to the DMPC membrane surface.[43,44] Similar results were obtained from our simulations, with a mean angle of 90° between the P−N vector and the *Z*-axis and 0° for the tail tilt angle. Since no significant differences were observed between the parameters obtained for the DMPC molecules in the center and boundaries of the systems, we conclude that no border effects or artifacts due to system size are present. In summary, the results obtained from simulations of DMPC membrane showed that our system was able to reproduce the structure of the real system in similar conditions of temperature, and therefore, the chosen simulation parameters were adequate for the study of DMPC bilayers.

TH−DMPC Complexes. The global parameters described in the previous section were also evaluated for the systems of DMPC membranes containing individual T4, T3d, T3p, and T2 molecules. No significant differences in the values concerning the surface area per DMPC molecule, number of *gauche* rotamers/chain, and tilt angles of head and tail groups were predicted between the DMPC membrane and TH−DMPC complexes. This showed that THs do not have a major impact on the overall structure of the bilayer, probably due to the low [TH]/[DMPC] ratio as well as the small molecular size of the hormones relative to the total system size.

Penetration of TH in the Lipid. A straightforward way of characterizing each TH−DMPC complex consists of evaluating the location of selected hormone atoms along the *Z*-axis and in relation to the average positions of specific lipid atoms, also along the *Z*-axis, as adopted during the simulations. Figure 2 shows the corresponding vertical locations of nitrogen (N), phosphorus (P), carbonyl oxygen (O), and methyl terminal

ohio2/yjp-yjp/yjp-yjp/yjp99907/yjp8202d07z | xppws | 23:ver.3 | 9/4/09 | 10:38 | Msc: jp-2009-055522 | TEID: jem00 | BATID: 00000

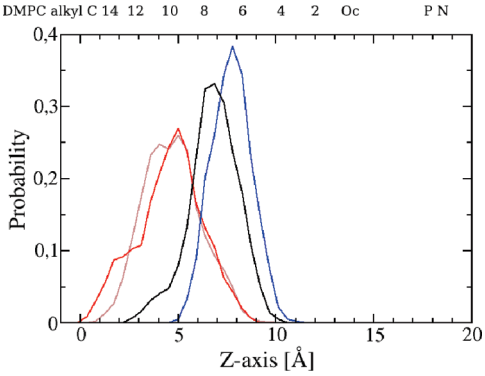

Figure 3. Distribution of the deepest atoms of THs in the membrane: distal H of T2 (brown), 3′ I of T3d (red) and T3p (blue), and distal I of T4 (black). The abscissa origin represents the hydrophobic core on the bilayer, while the polar heads of lipids are around the 18 Å scale. The average positions of C atoms of the alkyl chains with respect to the *Z*-axis are included.

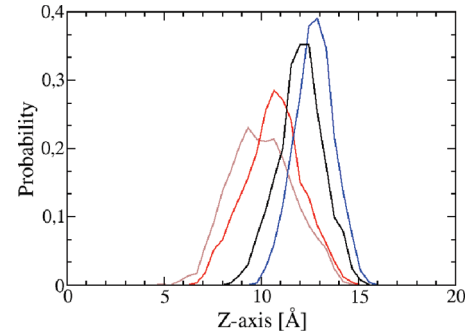

Figure 4. Probability of finding the geometric centers of THs, relative to the bilayer normal vector (*Z*-axis). T2 (brown), T3d (red), T3p (blue), and T4 (black). The abscissa origin represents the hydrophobic core on the bilayer, while the polar heads of lipids are around the 18 Å scale.

carbon (C) atoms of the DMPC molecules, together with the relative positions of the carboxylic carbon atom in the zwitterion group, the ether oxygen atom that connects both aromatic rings, and the oxygen atom of the phenol group in the hormone molecule, along the last 25 ns of the generated trajectories.

The graphics show that the hormones are immersed in the lipid medium, with their respective zwitterionic moieties in close interactions with the hydrophilic region of the phospholipids, while the phenol groups, and hence the β rings, are embedded in the alkyl chain region of the bilayer. In addition, a significant mobility of the THs is observed. A comparison among the four simulations shows that THs have different behaviors in the lipid medium, and it is summarized as follows: (i) The hormone T2 is the one that reaches the deepest in the lipid, in contrast to that observed for T3p, whose carboxylic group appears almost anchored in the membrane−water interface; (ii) both phenol and ether oxygen atoms in T3d and T4 get similar *Z*-axis values, while a constant difference of approximately 5 Å between these atoms is observed for T3p; (iii) T3p and T4 show that their carboxylic C, ether O, and phenol O atoms follow a similar pattern of fluctuation in each system, while the phenol O atoms in T2 and T3d show different behaviors with respect to those of the zwitterions and ether groups. This last observation shows that there is a degree of rigidity affecting the whole molecules of T4 and T3p. This is only restricted to the region involving α rings and zwitterion groups in T2 and T3d.

We evaluated the location with respect to the *Z*-axis adopted by the atom of the hormone closest to the lipid core during the last 20 ns of the trajectories to assess how far each TH is able to reach inside the bilayer. The corresponding results are shown in Figure 3. In T2, T3d, and T4, the deepest atom corresponds to the one in the ortho position of the phenol group, and in distal orientation with respect to the α ring (hydrogen in T2 and iodine in T3d and T4). In the case of T3p, the deepest atom in the lipid is the 3′ I in proximal orientation. Average *Z*-axis values (vertical position) for the C atoms of alkyl chains, as well as the carbonyl oxygen, phosphorus, and nitrogen atoms, all belonging to the lipid molecules are also included in Figure 3 for comparative purposes. The results show that T2 and T3d can go through one DMPC monolayer until the deepest atom is found close to the C10−C11 of the alkyl chains, while T4 gets to the level corresponding to the C8−C9 lipid atoms. Consistent with the previous analysis, T3p is the hormone with the lowest penetration inside the bilayer. Interestingly, unpublished results concerning EPR measurements using 5- and 10-deoxyl-stearate spin-labeled liposomes indicated that T2, T3, and T4 can disturb the lipid core region of the bilayer and perturb both spin probes (Farías, R. N. Private communication), suggesting that the THs are in close contact with C5 and C10 atoms of the lipid chain. Our MD simulation results are in agreement with those observations, even when no significant effects on the membrane structure upon TH incorporation are estimated from the simulations.

Mobility and Orientation of THs in the Lipid Medium. Fluctuations of the carbon geometric center of the hormone with respect to the *Z*-axis of the membrane give a clear idea of the vertical movement that each hormone displays inside the lipid bilayer. Figure 4 represents the mobility of the THs in terms of the distribution of each TH geometric center along the *Z*-axis during the last 20 ns of simulation. According to the position of the maximum and the width at half-height, the plot obtained for T2 indicates that it is the hormone with the highest probability of being closest to the core of the bilayer and also with the highest mobility. The comparison among the plots obtained for T2, T3d, and T4 evidences that the progressive iodine substitution on the β ring lowers both the possibility of penetration and the transversal mobility in the membrane. These results, together with the respective behaviors presented above, show that the iodine substitution on ring β plays a crucial role in the TH−lipid interactions, which is in agreement with previous results, indicating that the differential effects that THs produce in the membrane properties are strongly associated with the iodine content of the thyroid molecule analogues.[14−17] However, as shown in Figure 4, T3p presents the highest limitations in mobility and penetration in the lipid, staying apart from the aforementioned correlation between the hormone behavior and the degree of substitution in the phenolic ring. It follows then that the number of atoms of iodine in the molecule is not the unique factor in determining the capability of the hormone to penetrate the bilayers but also the position of the single iodine substitution on the β ring.

To further characterize the intrinsic TH structure inside the bilayer, the most probable orientation acquired by each TH in the lipid medium was characterized as a function of the angles formed between the *Z*-axis and the respective termed α, β, distal, and proximal vectors, as defined in the Computational Methods and shown in Figure 5. Table 1 lists the mean values calculated for these angles from the last 20 ns of simulations for the different TH−DMPC complexes. Figure 6 allows a visualization of these results by showing the most representative snapshots of the average orientations adopted by the THs in the lipid medium for each case.

The α and β angles calculated for the T2−DMPC complex indicate that the stabilization of the system is reached when

ohio2/yjp-yjp/yjp-yjp/yjp99907/yjp8202d07z | xppws | 23:ver.3 | 9/4/09 | 10:38 | Msc: jp-2009-055522 | TEID: jem00 | BATID: 00000

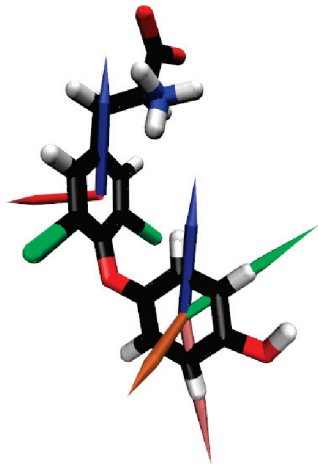

Figure 5. Representation of the normal vectors to α and β ring planes (in red and orange, respectively) and the vectors along the proximal and distal molecular bonds (in green and pink, respectively) in T2. The *Z*-axis (normal to the membrane surface), shown in blue, is also included to define the respective angles formed between this coordinate and the vectors that characterize the orientation of the hormone in the lipid.

TABLE 1: Locations and Orientations of TH in the DMPC Bilayer

	T2-DMPC	T3d-DMPC	T3p-DMPC	T4-DMPC
α angle[a] (deg)	92 ± 9	104 ± 7	26 ± 9	113 ± 7
β angle[b] (deg)	84 ± 14	83 ± 11	84 ± 10	75 ± 10
distal angle[c] (deg)	160 ± 8	162 ± 7	101 ± 10	154 ± 9
proximal angle[d] (deg)	61 ± 10	52 ± 8	136 ± 10	44 ± 8
zwitterion group[e]	*cis*	*cis*	*trans*	*cis*

[a] Angle defined by the normal vector to the plane of ring α with the *Z*-axis. [b] Angle defined by the normal vector to the plane of ring β with the *Z*-axis. [c] Angle defined by the vector containing the distal C−H bond (T2, T3p) or distal C−I bond (T3d, T4) with the *Z*-axis. [d] Angle defined by the vector containing the proximal C−H bond (T2, T3d) or proximal C−I bond (T3p, T4) with the *Z*-axis. [e] Orientation of the zwitterion group with respect to ring β.

both rings are oriented almost parallel to the *Z*-axis (since the normal vectors form angles of 92 and 84° with the *Z*-axis, respectively), and that the distal C−H bond is nearly parallel to the *Z*-axis (160°). Consistently, the distal H atom is the one reaching the deepest part of the bilayer. On the other hand, the interconversion between *cis* and *trans* orientations of the zwitterion group with respect to the β ring is strongly limited for the hormone in the lipid. As a result, the *cis* conformation is the preferred structure. By considering the orientation adopted by T2 as a reference, the orientations of the other THs can be interpreted in terms of the different iodine substitution on the β ring. Thus, for the system T3d−DMPC, a slight increment of the α angle is observed, while the orientation of the β ring remains unchanged. This last point is particularly relevant, since it implies that the distal C−I bond is almost parallel to the *Z*-axis and directed toward the bilayer core, favoring the minimum spatial interaction between the iodine atom with the lipid chains (Figure 6B). When two iodine substituents are present in the phenolic ring (T4), the spatial disposition of this ring is slightly different due to the fact that both C−I bonds attempt to decrease their steric interactions with the alkyl groups (Figure 6D). This change is naturally accompanied by a change in the orientation of the α angle which is moved away from the perpendicularity with respect to the *Z*-axis.

The most significant effect of the iodine substitution in the β ring is observed for T3p. In this case, the system acquires stability by directing the 3′-I bond toward the core of the bilayer instead of directing it toward the polar region of the lipids, as is the case of the proximal I atom in the T4−DMPC complex. Thus, while the C−I bond in the β ring of T3p minimizes the interaction with the alkyl chains, a significant reorientation of the rest of the molecule is forced, resulting in an almost perpendicular disposition of the α ring with respect to the *Z*-axis (α angle = 26°), and a rotation of the zwitterion group by approximately 180° in order to adopt a *trans* conformation. As a result of such unfavorable orientation of the α ring, it is expected that the T3p will have a low capacity to penetrate inside the bilayer, as well as a low transversal mobility in the lipid medium. The location of the oxygen atom of the ether group with respect to the *Z*-axis along the simulation time (Figure 2C) and the plot obtained from the fluctuations of the geometric center of T3p in the direction of the normal vector to the bilayer (Figure 4) support these arguments.

Structural Changes in the Hormone Molecules upon Lipid Incorporation. The interest in analyzing the TH−lipid interactions on a molecular level was also focused on the hormone conformational changes induced by the membrane environment. Several structural parameters were measured for each TH in solution and in the TH−DMPC complexes in order to analyze the changes in the TH structures upon lipid interaction. Specific attention was paid to the orientation of the aromatic rings with respect to each other, as described by the angle between the normal to each ring and the normal to the plane through the three atoms of the ether linkage. Additionally, the C−O−C ether linkage angle was also evaluated. Figure 7 shows the corresponding parameters for the THs in water and in DMPC resulting from the respective simulations. MD simulations of THs in water supply the reference values for these angles and show that the mutual orientation of the aromatic rings results in a perpendicular orientation for ring α and a parallel orientation for ring β with respect to the ether bridge plane (α ring, ether plane dihedral angle ∼90°; β ring, ether plane dihedral angle ∼0°, respectively, as shown in Figure 1A). Similar results are obtained for all THs independent of the presence of iodine atoms in the phenolic ring. The C−O−C angle is also similar for the four hormone molecules in water, displaying a value close to the expected 120°. The changes in the ether bridge angles are negligible for the four hormone molecules in the different environments. The orientations of the α ring with respect to the ether plane in T2, T3d, and T3p show slight deviations (not higher than 3°), and only a distortion of approximately 7° is obtained for T4 when the hormone is transferred from the water to the lipid medium. The change in the mutual orientation of the rings upon insertion of THs in the lipid can be considered as a direct consequence of the deviations from the coplanarity between the β ring and the ether plane, showing values of approximately 8° (T3p), 10° (T2), 11° (T3d), and 16° (T4). These data clearly indicate that main structural changes upon insertion in the membrane involve the beta ring. The structural changes obtained from the simulations are in good agreement with previous Raman spectroscopic studies on the conformational changes of T3 and T4 induced by interactions with phospholipids,[18,19] which reported that essentially all of the spectral changes observed in the Raman spectra of T3/PC and T4/PC complexes refer to modes that are localized mainly in the β ring and the ether bridge. In addition, the magnitude of the spectral changes observed for T4 upon lipid interaction[18] is in concordance with the major conformational changes derived from the dynamic simulations, while a higher flexibility around the ether linkage was predicted by quantum-chemical calcula-

ohio2/yjp-yjp/yjp-yjp/yjp99907/yjp8202d07z | xppws | 23:ver.3 | 9/4/09 | 10:38 | Msc: jp-2009-055522 | TEID: jem00 | BATID: 00000

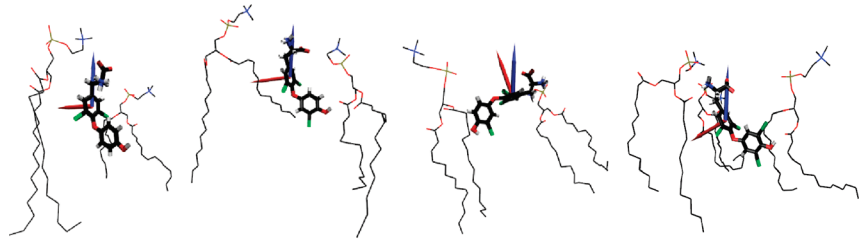

Figure 6. Selected snapshots of the different TH−DMPC complexes showing the most probable orientation of the hormones in the lipid: (A) T2; (B) T3d; (C) T3p; (D) T4. The *Z*-axis vector (in blue) and the normal vector to the plane of ring α (in red) are shown as a reference.

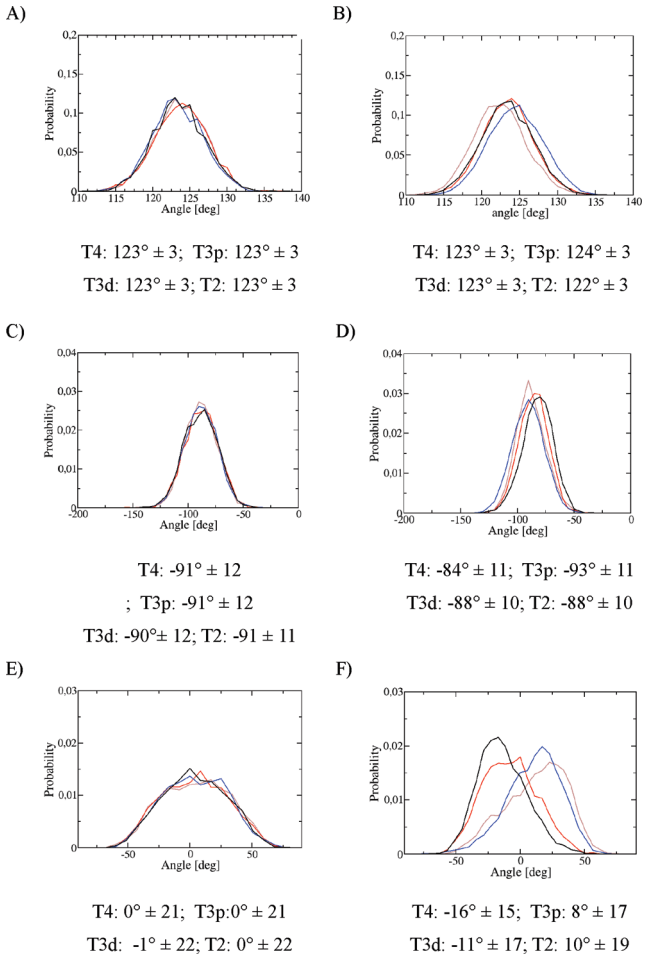

Figure 7. Distribution of specific molecular parameters of THs in water and in the DMPC lipid: C−O−C ether bridge angle (A, in water; B, in the membrane); α ring, ether plane dihedral angle (C, in water; D, in the membrane), and *β* ring, ether plane dihedral angle (E, in water; F, in the membrane). The corresponding average values are included. T2 (brown), T3d (red), T3p (blue), and T4 (black).

tions for T3d in comparison with T3p,[19] showing also good correlation with the simulated conformational changes.

TH Interactions with DMPC and Water Molecules. From the previous section, it is derived that an important factor in the stabilization of the TH−DMPC systems is the interaction between the zwitterion moiety of the hormone with the polar head of the lipids and with the water molecules in the membrane surface. In order to identify the most relevant electrostatic interactions in this hydrophilic region, radial distribution functions were computed considering several interacting atoms: (i) Carboxylic oxygen atom (Oz) of the zwitterion group with the quaternary nitrogen (Nq) of the DMPC choline groups around the hormone, (ii) nitrogen atom (Nz) of the zwitterion group

TABLE 2: Radial Distribution Functions between Different Interacting Atoms, Distance (*r* (Å)), and Integral Area (Int) of the First Maximum

	T2		T3d		T3p		T4	
	r	Int	*r*	Int	*r*	Int	*r*	Int
$R-CO_2^-$ $N(CH_3)_3^+$	4.1	0.82	4.4	0.57	4.5	0.63	4.0	0.66
$R-CO_2^-$ H_2O	2.8	2.49	2.8	2.48	2.8	2.59	2.8	2.44
$R-NH_3^+$ H_2O	3.0	2.49	3.0	3.01	3.0	2.85	3.0	0.46
$R-NH_3^+$ PO_2^-	2.9	0.97	2.9	1.30	2.9	0.82	2.9	1.85
$R-NH_3^+$ C═O	2.9	0.48			3.0	0.24	3.0	0.95

with the nonester phosphate oxygen atoms (Op) of the DMPC neighbor molecules, (iii) nitrogen atom (Nz) of the zwitterion group with the carbonyl oxygen atoms (Oc) of the DMPC neighbor molecule, and (iv) carboxylic oxygen atom (Oz) and nitrogen atom (Nz) of the hormone with the oxygen (Ow) of water molecules on the membrane surface.

The results of these radial distribution functions, computed for each TH−DMPC system, are collected in Table 2. All of the functions have an intense and well-defined maximum at distances corresponding to hydrogen bond interactions (2.8−3.0 Å) or electrostatic interactions (4.0−4.5 Å). The integration areas of these peaks are interpreted as the mean number of specific neighbors interacting with the selected hormone atom (occupancy).

The *g*(*r*) values obtained for the interactions of Oz and Nz with Ow indicate that the zwitterion moieties of HTs are well solvated with superficial water molecules. Both groups, CO_2^- and NH_3^+ in T2, T3d, and T3p can set up to 5.5 hydrogen bond interactions with the surrounding water molecules, while T4 is involved only in three associations of this type. The Oz atoms of hormones are also able to participate in electrostatic interactions with the $N(CH_3)_3^+$ choline group. In general, no significant differences are predicted for the interactions of the CO_2^- group among the four TH−DMPC systems. As far as the NH_3^+ group is concerned, additional hydrogen bonds with the lipid P═O and C═O groups are expected. In addition, important variations in the respective integration areas are observed when the four simulated systems are compared. Assuming that the interactions involving the donor NH_3^+ group are competitive, the interpretations of these differences are straightforward. The intensity of the peak corresponding to the Nz−Op interaction in the T4−DMPC complex is approximately the double of those estimated for the remaining hormones (Figure 8A), while the strength of the interaction Nz−Oc decreases conforming T4 ≫ T2 > T3p > T3d (Figure 8B). However, as it has been mentioned, T4 shows only a few interactions by hydrogen bonds with water molecules, which is supported by the weak intensity of the peak calculated for Nz−Ow interaction (Figure 8C). Similarly, radial distribution functions calculated for the T3d−DMPC complex point out that the negligible Nz−Oc interaction appears compensated by the number of Nz−Ow

ohio2/yjp-yjp/yjp-yjp/yjp99907/yjp8202d07z | xppws | 23:ver.3 | 9/4/09 | 10:38 | Msc: jp-2009-055522 | TEID: jem00 | BATID: 00000

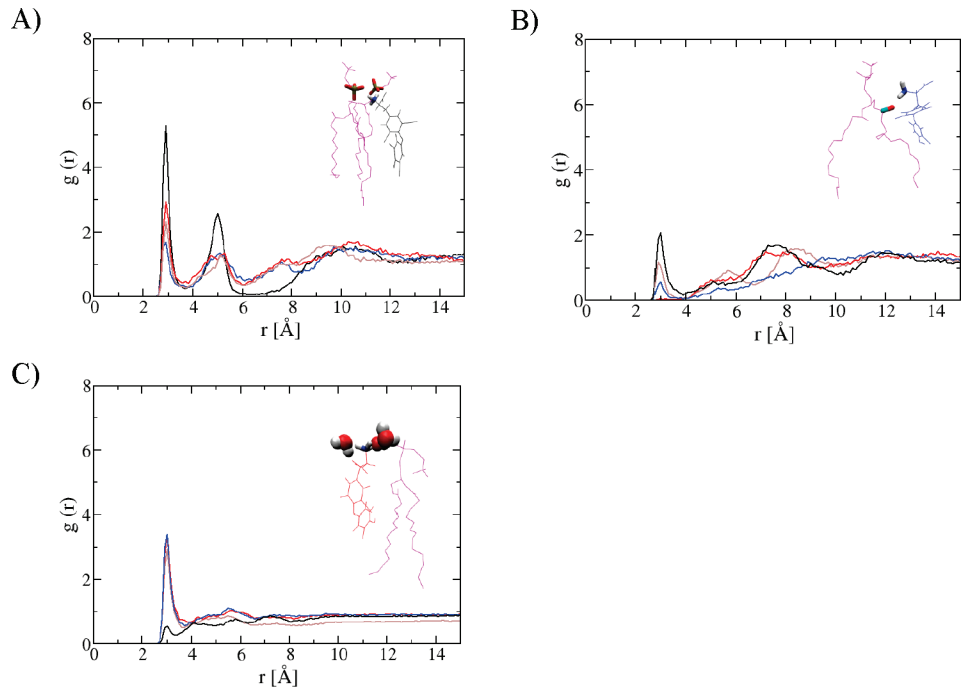

Figure 8. Op (A), Oc (B), and Ow (C) radial distribution functions for the nitrogen of the THs. T2 (brown), T3d (red), T3p (blue), and T4 (black). The insets show selected snapshots, showing interactions corresponding to the first peak in each graphic (DMPC lipid is shown in purple).

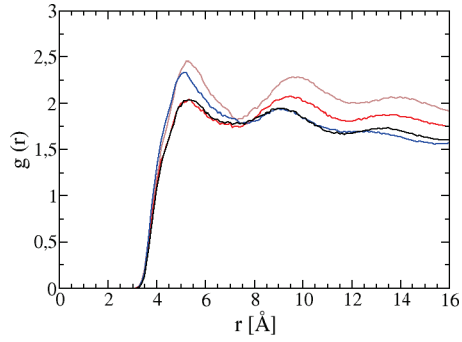

Figure 9. Radial distribution functions of the carbon atoms of DMPC alkyl chains relative to the β ring of thyroid hormones in the complexes: T2-DMPC (brown), T3d-DMPC (red), T3p-DMPC (blue), and T4-DMPC (black).

hydrogen bond interactions with interfacial water molecules. The results altogether show that TH charged groups strongly interact with either the water molecules or polar groups of the membrane.

Packing of DMPC Lipid around Hormone. Radial distribution functions of the alkyl carbon atoms relative to the β ring provide information related to the interactions that occur in the hydrophobic region of the TH−DMPC complexes and to the organization of the alkyl chains around the hormone aromatic rings. Figure 9 compares the calculated $g(r)$ for the four systems. In all cases, there are two well-defined maxima, indicating that the DMPC alkyl chains adopt a nonrandom distribution around the β rings of hormones. The first maxima are approximately at 5 Å, corresponding to van der Waals interactions between the carbon atoms integrating the β ring and the lipid hydrocarbon chains. Significant differences are observed in the values of the respective $g(r)$, showing that the presence of iodine atoms modifies the density of alkyl chains in the vicinities of the ring. T2 presents the highest packing of atoms around the β ring, in accordance with the absence of iodine; the number of neighboring carbon atoms in T3d−DMPC and T4−DPMC complexes is considerable lower than that in T2. However, the most interesting observation concerns the high density of alkyl chains around the β ring of T3p. This fact is rationalized in terms of the orientation adopted by the T3p molecule in the lipid, which results in a lower exposition of the 3′-I atom to the alkyl chains favoring van der Waals interactions between the carbon atoms (see Figure 6C). The second maxima (Figure 9) show differences in the $g(r)$ values as well as in the distances from the β ring carbon atoms (centered in the range between 9 and 10 Å) and also in relation to the hormone orientation in the membrane. Thus, T4 and T3p have low densities of alkyl chains compared with T2 and T3d, which have their α ring planes oriented almost parallel to the normal to the bilayer decreasing the area of chains exclusion around the phenolic ring.

The presence of two iodine atoms in the phenolic ring of T4 produces the lowest global condensing effect of alkyl chains in the vicinity of the hormone compared with T2, T3d, and T3p. However, the van der Waals interactions between the methylene groups of DMPC alkyl chains and the aromatic ring of T4 are still of significant magnitude, contrarily to that reported for the cholesterol effect in DMPC−Chol bilayers where the interactions involving the steroid rings are weak.[22]

Conclusions

In summary, the data obtained from the simulation made it possible to perform a consistent analysis of local interactions between functional groups of hormone and hydrophobic/hydrophilic regions of the lipid membrane. The results obtained for T2, T3d, and T4 indicate that the number of iodine atoms in the β ring is determinant in both the depth penetration accomplished and the orientation adopted by the hormone in the lipid medium. However, the orientation of the single iodine substitution of the β ring regarding the α ring is also a relevant factor in the hormone behavior, as it is derived from the simulations of the T3p−DMPC complex. In all of the cases, it has been observed that the hormones accomplish better adaptation to the medium by reorientations of the phenolic ring.

In addition, the results presented here show good concordance with those previously obtained by experimental methods[18,19] and

the following correlations between them are proposed: first, the simulations clearly show that the deepest atoms in T2 and T3d attain the positions C10−C11 of the alkyl chains, while in the T4, the position close to C8−C9 is reached. These results correlate with the spectroscopic data, since most of the spectral changes observed in the Raman spectra of the hormone−lipid complexes refer to modes localized in the β ring and the ether bridge, pointing out that this moiety is close to the lipid core. On the other hand, preliminary EPR measurements using spin-labeled liposomes indicated that T2, T3, and T4 disturb the lipid core region and perturb the probes localized at C5 and C10 of the alkyl chain. Second, the simulations show that the hormones are immersed in the lipid medium with the β rings embedded in the alkyl chain region of the bilayer, in agreement with the Raman vibrational analyses of T3 and T4 bound to PC membranes, which point out that the β ring, the ether linkage, and a part of the α ring of THs are anchored between the aliphatic chains of the lipid via hydrophobic interactions. Third, conformational changes affecting almost exclusively the mutual orientation of the aromatic rings were derived from the Raman frequency shifts. In addition, a bigger deviation from the coplanarity involving the β ring and the ether bridge was assumed for T4 based on the magnitude of the spectral changes, in comparison with the structural changes estimated for both conformers of T3 in the lipid medium. Indeed, the simulations predict that the major molecular distortions are experienced by T4. Finally, both the structural changes of the hormone molecules upon lipid interaction derived from the simulations and the depth reached by the THs in the membrane agree with previous quantum-chemical optimizations of T3d and T3p in different solvents, which concluded that the distal form presents a higher flexibility around the ether bridge. This property, together with the characteristic geometrical parameters, would allow a better accommodation of the T3d into the membrane compared to T3p and T4.

The present computational approach to the study of TH−lipid interactions helps us gain an insight into the different effects that thyroxine and its analogues distal and proximal 3,5,3′-triiodothyronine and 3,5-diiodothyronine produce on the physicochemical properties of the membranes and supports conclusions previously derived from vibrational and conformational studies focused on the molecular properties of the hormones.

Acknowledgment. This work was partially supported by CONICET, National University of Tucumán, and Grants PICT 2007-01650 and UBA08-X625 to M.A.M. A.A.P. is grateful to CONICET for a Doctoral Fellowship. Computer power was gently provided by the CECAR at FCEN-UBA and by Open Science Grid supported by NSF and the US Department of Energy's Office for Science. We also thank Prof. Dr. Ricardo Farías for helpful discussions and Prof. Lic. Betty Omega for her helpful orientation on the computational analysis of the data. M.A.M. and R.M.S.A. are members of CONICET.

References and Notes

(1) Pinna, G.; Meinhold, H.; Hiedra, L.; Thoma, R.; Hoell, T.; Gräf, K. J.; Stoltenburg-Didinger, G.; Eravci, M.; Prengel, H.; Brödel, O.; Finke, R.; Baumgartner, A. *J. Clin. Endocrinol. Metab.* **1997**, *82*, 1535–1542.

(2) Silvestri, E.; Schiavo, L.; Lombardi, A.; Goglia, F. *Acta Physiol. Scand.* **2005**, *184*, 265–283.

(3) Davis, P. J.; Davis, F. B.; Cody, V. *Trends Endocrinol. Metab.* **2005**, *16*, 429–435.

(4) Hulbert, A. *J. Biol. Rev.* **2000**, *75*, 519–631.

(5) Schreiber, G.; Richardson, S. J. *Comp. Biochem. Physiol., B* **1997**, *116*, 137–160.

(6) Visser, W. E.; Frieseman, E. C. H.; Jansen, J.; Visser, T. J. *Trends Endocrinol. Metab.* **2008**, *19* (2), 50–56.

(7) Hennemann, G.; Docter, R.; Frisema, E. C. H.; De Jong, M.; Krenning, E. P.; Visser, T. *J. Endocrinol. Rev.* **2001**, *22*, 451–476.

(8) Taylor, P. M.; Ritchie, J. W. A. *Best Pract. Res. Clin. Endocrinol. Metab.* **2007**, *21*, 237–251.

(9) Abe, T.; Suzuki, T.; Unno, M.; Tokui, T.; Ito, S. *Trends Endocrinol. Metab.* **2002**, *13*, 215–220.

(10) Robbins, J.; Rall, J. E. *Physiol. Rev.* **1960**, *40*, 415–489.

(11) Lai, C.-S.; Cheng, S.-Y. *Biochim. Biophys. Acta* **1982**, *692*, 27–32.

(12) Lai, C.-S.; Cheng, S.-Y. *Arch. Biochem. Biophys.* **1984**, *232*, 477–481.

(13) Lai, C.-S.; Korytowski, W.; Niu, C.-H.; Cheng, S.-Y. *Biochem. Biophys. Res. Commun.* **1985**, *131*, 408–412.

(14) Cheihn, R. N.; Rintoul, M. R.; Morero, R. D.; Farias, R. N. *J. Membr. Biol.* **1995**, *147*, 217–221.

(15) Chehín, R. N.; Issé, B. G.; Rintoul, M. R.; Farías, R. N. *J. Membr. Biol.* **1999**, *167*, 251–256.

(16) Farías, R. N.; Chehin, R. N.; Rintoul, M. R.; Morero, R. D. *J. Membr. Biol.* **1995**, *143*, 135–141.

(17) Issé, B.; Fidelio, G.; Farías, R. N. *J. Membr. Biol.* **2003**, *191*, 209–213.

(18) Álvarez, R. M. S.; Della Védova, C. O.; Mack, H. G.; Farías, R. N.; Hildebrandt, P. *Eur. Biophys. J.* **2002**, *31*, 448–453.

(19) Álvarez, R. M. S.; Cutin, E. H.; Farías, R. N. *J. Membr. Biol.* **2005**, *205*, 61–69.

(20) Camerman, A.; Camerman, N. *Acta Crystallogr.* **1974**, *B30*, 1832–1840.

(21) Duggan, B. M.; Craik, D. J. *J. Med. Chem.* **1996**, *39*, 4007–4016.

(22) Róg, T.; Pasenkiewicz-Gierula, M. *FEBS Lett.* **2001**, *502*, 68–71.

(23) Róg, T.; Pasenkiewicz-Gierula, M. *Biophys. J.* **2003**, *84*, 1818–1826.

(24) Hoff, B.; Strandberg, E.; Ulrich, A. S.; Tieleman, D. P.; Posten, C. *Biophys. J.* **2005**, *88*, 1818–1827.

(25) Róg, T.; Pasenkiewcz-Gierula, M.; Vattulinen, I.; Karttunen, M. *Biophys. J.* **2007**, *92*, 3346–3357.

(26) Barrachina, I.; Royo, I.; Baldoni, H. A.; Chahboune, N.; Suvire, F.; DePedro, N.; Zafra-Polo, M. C.; Bermejo, A.; El Aouad, N.; Cabedo, N.; Saez, J.; Tormo, J. R.; Enriz, R. D.; Cortes, D. *Bioorg. Med. Chem.* **2007**, *15*, 4369–4381.

(27) Róg, T.; Stimson, L. M.; Pasenkiewicz-Gierula, M.; Vattulainen, I.; Karttunen, M. *J. Phys. Chem. B* **2008**, *112*, 1946–1952.

(28) MacCallur, J. L.; Bennett, W. F. D.; Tieleman, D. P. *Biophys. J.* **2008**, *94*, 3393–3404.

(29) Law, R. J.; Tieleman, D. P.; Sansom, M. S. P. *Biophys. J.* **2003**, *84*, 14–27.

(30) Villarreal, M. A.; Perduca, M.; Monaco, H. L.; Montich, G. G. *Biochim. Biophys. Acta* **2008**, *1778* (6), 1390–1397.

(31) Feller, S. E.; Venable, R. M.; Pastor, R. W. *Langmuir* **1997**, *13*, 6555–6561.

(32) Feller, S.; MacKerell, A. D., Jr. *J. Phys. Chem. B* **2000**, *104*, 7510–7515.

(33) Wang, J.; Cieplak, P.; Kollman, P. A. *J. Comput. Chem.* **2000**, *21*, 1049–1074.

(34) Frisch, M. J.; Trucks, G. W.; Schlegel, H. B.; Scuseria, G. E.; Robb, M. A.; Cheeseman, J. R.; et al. *Gaussian 03*, revision A.I; Gaussian: Pittsburgh, PA, 2003.

(35) Wang, J.; Wolf, R. M.; Caldwell, J. W.; Kollamn, P. A.; Case, D. A. *J. Comput. Chem.* **2004**, *25*, 1157–1174.

(36) Case, D. A.; Darden, T. A.; Cheartham,T. E., Jr.; Simmerling, C. L.; Wang, J.; Duke, R. E.; Luo, R.; Merz, K. M.; Pearlman, D. A.; Crowley, M.; Walker, R. C.; Zhang, W.; Wang, W.; Hayik, S.; Roitberg, A.; Seabra, G.; Wong, K. F.; Paesani, F.; Wu, X.; Brozell, S.; Tsui, V.; Gohlke, H.; Yang, L.; Tan, C.; Mongan, J.; Hornak, V.; Cui, G.; Beroza, P.; Mathews, D. H.; Schafmeister, C.; Ross, W. S.; Kollman P. A. *AMBER 9*; University of California: San Francisco, CA, 2006.

(37) Ryckaert, J. P.; Ciccotti, G.; Berendsen, H. J. C. *J. Comput. Phys.* **1977**, *23*, 327–341.

(38) Berendsen, H. J. C.; Postma, J. P. M.; van Gunsteren, W. F.; DiNola, A.; Haak, J. R. *J. Chem. Phys.* **1984**, *81*, 3684–3690.

(39) Humphrey, W.; Dalke, A.; Schelten, K. *J. Mol. Graphics* **1996**, *14*, 33–38.

(40) Petrache, H. I.; Steven, W. D.; Brown, M. F. *Biophys. J.* **2000**, *79*, 3172–3192.

(41) Pink, D. A.; Green, T. J.; Chapman, D. *Biochemistry* **1980**, *19*, 349–356.

(42) Büldt, G.; Gally, H. U.; Seelig, J. *J. Mol. Biol.* **1979**, *134*, 673–691.

(43) Moser, M.; Mash, D.; Meier, P.; Wassmer, K.-H.; Kolthe, G. *Biophys. J.* **1989**, *55*, 111–123.

(44) Meier, P.; Blume, A.; Ohmes, E.; Neugebauer, F. A.; Kithe, G. *Biochemistry* **1982**, *21*, 526–534.

JP9055522